

Supplementary Material

Three-Dimensional MoS₂/Reduced Graphene Oxide Nanosheets/Graphene Quantum Dots Hybrids for High-Performance Room-Temperature NO₂ Gas Sensors

Cheng Yang ^{1,2}, Yanyan Wang ^{1,2,*}, Zhekun Wu ^{1,2}, Zhanbo Zhang ^{1,2}, Nantao Hu ^{3,*} and Changsi Peng ^{1,2}

- ¹ School of Optoelectronic Science and Engineering & Collaborative Innovation Center of Suzhou Nano Science and Technology, Soochow University, Suzhou 215006, China; 20205239020@stu.suda.edu.cn (C.Y.); 20185208036@stu.suda.edu.cn (Z.W.); 20205239028@stu.suda.edu.cn (Z.Z.); changsipeng@suda.edu.cn (C.P.)
- ² Key Lab of Advanced Optical Manufacturing Technologies of Jiangsu Province & Key Lab of Modern Optical Technologies of Education Ministry of China, Soochow University, Suzhou 215006, China
- ³ Key Laboratory of Thin Film and Microfabrication (Ministry of Education), Department of Micro/Nano Electronics, School of Electronic Information and Electrical Engineering, Shanghai Jiao Tong University, Shanghai 200240, China
- * Correspondence: yywang@suda.edu.cn (Y.W.); hunantao@sjtu.edu.cn (N.H.)

The formation of MoS₂/rGO/GQDs hybrids was noticeable from the AFM image in Fig. S1, from which the spots corresponding to the GQDs were clearly observed on the exterior surface of the pristine MoS₂/rGO.

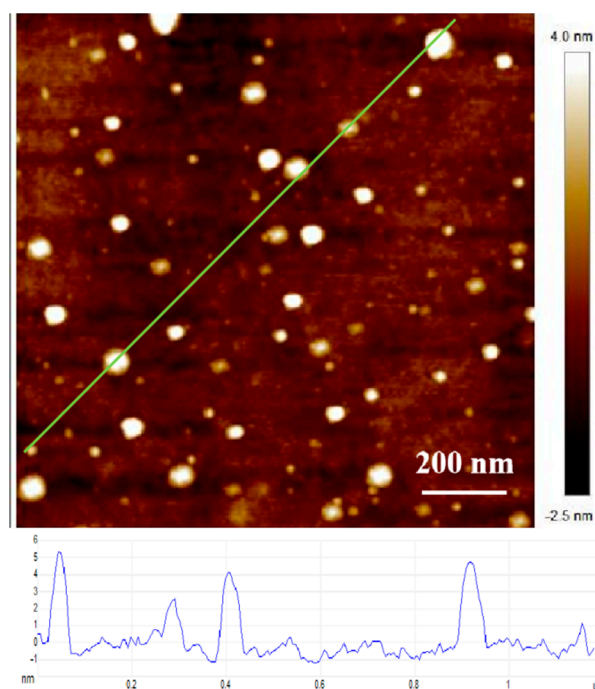


Figure S1. AFM image of MoS₂/rGO/GQDs.

Fig. S2 shows the morphologies of MoS₂/rGO/GQDs hybrids with different ratios of GQDs (MoS₂/rGO/GQDs hybrids with mass ratios of 50:10:10, 50:5:5, 50:3:3, and 50:2:2, denoted as MoS₂/rGO/GQDs-1, MoS₂/rGO/GQDs-2, MoS₂/rGO/GQDs-3, and MoS₂/rGO/GQDs-4, respectively). When the ratio of MoS₂, rGO and GQDs was 50:10:10, the dispersion of MoS₂/rGO/GQDs-1 hybrids was relatively uniform and MoS₂ nanoflowers combined closely with rGO nanosheets, without obvious agglomeration. When the ratio of MoS₂, rGO and GQDs was 50:5:5, numerous small MoS₂ nanoflowers were evenly distributed on the surface of rGO nanosheets in MoS₂/rGO/GQDs-2 hybrids. When the ratio of MoS₂, rGO and GQDs was 50:3:3, MoS₂ nanoflowers tended to aggregate in MoS₂/rGO/GQDs-3 hybrids. As the content of GQDs in the hybrids further decreased, MoS₂ nanosheets showed severe aggregation and overlapping. This caused an increase in the size of the formed MoS₂ nanoflowers and reduced the dispersion of the hybrids. The experimental results indicated that the microstructures of MoS₂/rGO/GQDs hybrids were significantly affected by the ratio of MoS₂, rGO and GQDs. As seen from Fig. S2, the addition of GQDs limited the aggregation of MoS₂ nanosheets, which caused a decrease in the size of MoS₂ nanoflowers. Numerous active sites and transportation channels were likely formed due to the small MoS₂ nanosheets, which contributed to the gas adsorption property. The MoS₂/rGO/GQDs-2 composite material exhibited better dispersion than the other hybrids and was selected for further study.

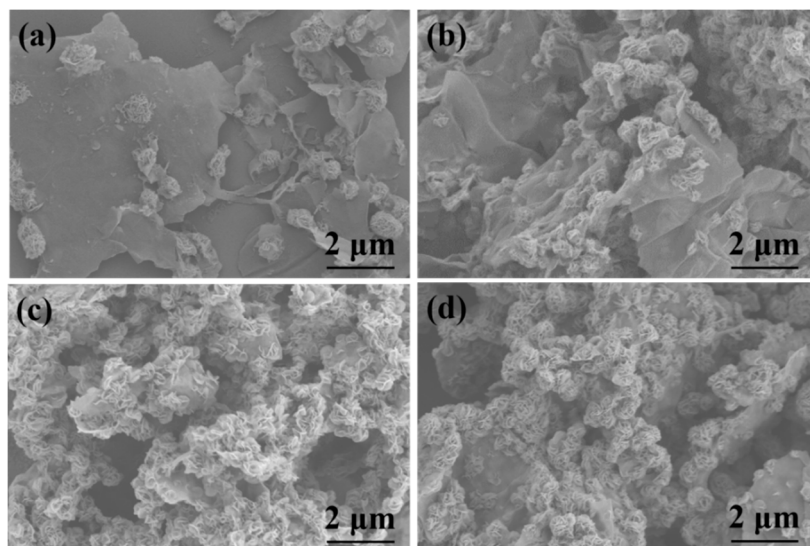


Figure S2. SEM images of (a) MoS₂/rGO/GQDs-1, (b) MoS₂/rGO/GQDs-2 (c) MoS₂/rGO/GQDs-3 and (d) MoS₂/rGO/GQDs-4.

CV tests were carried out in an aqueous solution of KCl and K₃Fe(CN)₆ to confirm whether the surface area increased after the addition of GQDs (Fig. S3). 200 μg of MoS₂/rGO nanocomposites and 200 μg of MoS₂/rGO/GQDs hybrids were uniformly coated on a 1 cm × 1 cm indium-tin-oxide (ITO) anode respectively for the CV test. The effective surface area can be calculated from the Randles-Sevcik equation [64]:

$$i_p = (2.687 \times 10^5) n^{3/2} v^{1/2} D^{1/2} AC$$

Where i_p refers to the peak current, n is the number of electrons transferred in the redox process ($n = 1$, in 10 mM K₃Fe(CN)₆), v is the scan rate, D is the diffusion coefficient ($D = 5.7 \times 10^{-6} \text{ cm}^2 \text{ s}^{-1}$, in 0.1 M KCl), A is the surface are and C is the concentration of K₃Fe(CN)₆. As shown in Fig. S4, the peak current i_p and the square root of scan rate v for both MoS₂/rGO/GQDs hybrids (slope = 14.455) and MoS₂/rGO nanocomposites (slope = 7.475). Moreover, the effective surface area of MoS₂/rGO/GQDs hybrids and MoS₂/rGO nanocomposites were calculated to be 2.253 and 1.165 cm², respectively, indicating the significant enhancement of effective surface area with the addition of GQDs [65,66].

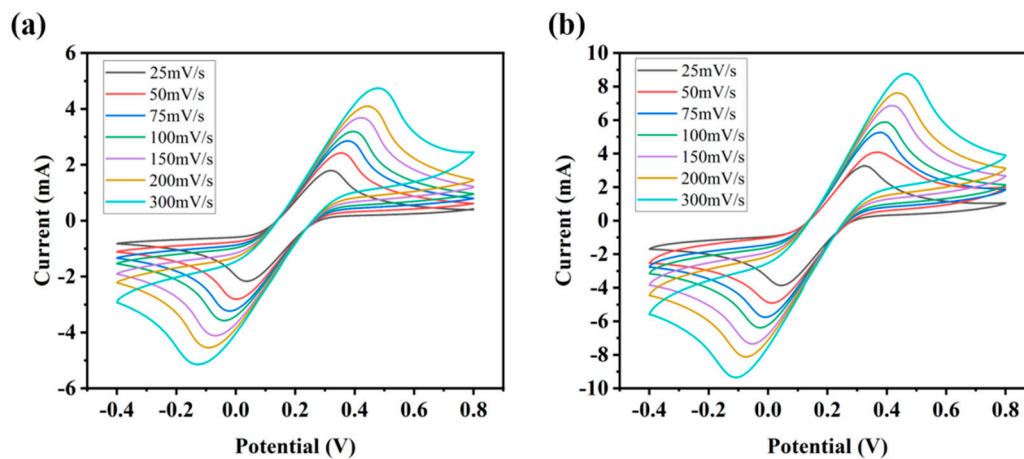


Figure S3. Cyclic voltammograms of (a) MoS₂/rGO nanocomposites and (b) MoS₂/rGO/GQDs hybrids in 10 mM [Fe(CN)₆]^{3-/4-} and 0.1 M KCl solution at different scan rates from 25 to 300 mV·s⁻¹.

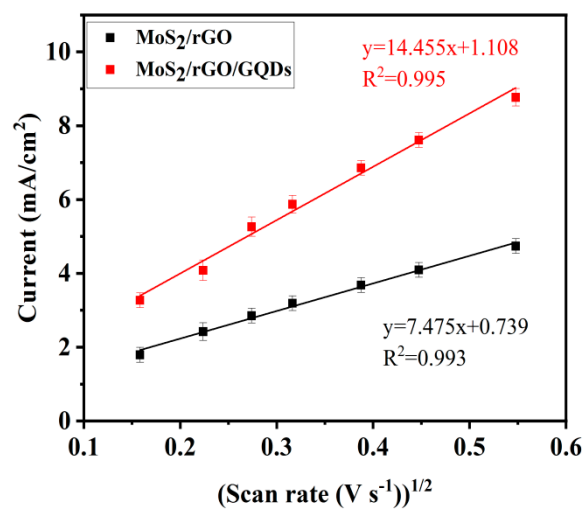


Figure S4. Peak currents as a function of scan rate for the determination of the effective surface area.

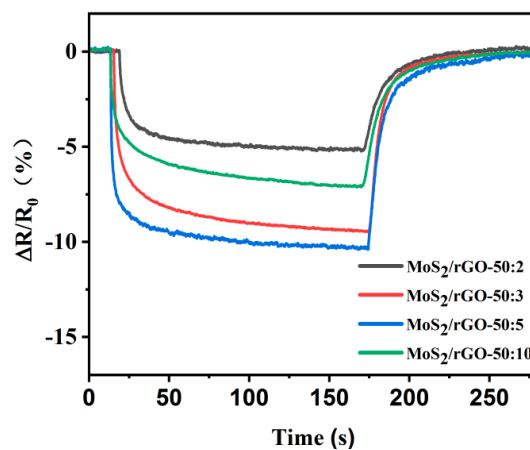


Figure S5. Response and recovery curves of MoS₂/rGO-based sensors to 5 ppm NO₂.